Plant Diversity 46 (2024) 395–405

Contents lists available at ScienceDirect

Plant Diversity

journal homepage: http://www.keaipublishing.com/en/journals/plant-diversity/
http://journal.kib.ac.cn

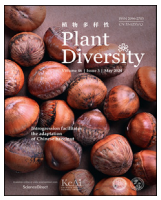

Research paper

Stomatal dynamics are regulated by leaf hydraulic traits and guard cell anatomy in nine true mangrove species

Ya-Dong Qie [a, b], Qi-Wei Zhang [c, d], Scott A.M. McAdam [e], Kun-Fang Cao [a, b, *]

[a] State Key Laboratory for Conservation and Utilization of Subtropical Agro-Bioresources, College of Forestry, Guangxi University, Nanning 530004, China
[b] Guangxi Key Laboratory of Forest Ecology and Conservation, College of Forestry, Guangxi University, Nanning 530004, China
[c] Key Laboratory of Ecology of Rare and Endangered Species and Environmental Protection, Ministry of Education, Guangxi Normal University, Guilin 541001, China
[d] Guangxi Key Laboratory of Landscape Resources Conservation and Sustainable Utilization in Lijiang River Basin, Guangxi Normal University, Guilin 541001, China
[e] Purdue Center for Plant Biology, Department of Botany and Plant Pathology, Purdue University, West Lafayette, IN 47907, USA

ARTICLE INFO

Article history:
Received 13 October 2023
Received in revised form
4 January 2024
Accepted 5 February 2024
Available online 8 February 2024

Keywords:
Stomatal temporal kinetics
Vapour-pressure deficit (VPD)
Leaf water relations
Leaf hydraulic vulnerability
Leaf osmotic potential
Genome size

ABSTRACT

Stomatal regulation is critical for mangroves to survive in the hyper-saline intertidal zone where water stress is severe and water availability is highly fluctuant. However, very little is known about the stomatal sensitivity to vapour pressure deficit (VPD) in mangroves, and its co-ordination with stomatal morphology and leaf hydraulic traits. We measured the stomatal response to a step increase in VPD *in situ*, stomatal anatomy, leaf hydraulic vulnerability and pressure-volume traits in nine true mangrove species of five families and collected the data of genome size. We aimed to answer two questions: (1) Does stomatal morphology influence stomatal dynamics in response to a high VPD in mangroves? with a consideration of possible influence of genome size on stomatal morphology; and (2) do leaf hydraulic traits influence stomatal sensitivity to VPD in mangroves? We found that the stomata of mangrove plants were highly sensitive to a step rise in VPD and the stomatal responses were directly affected by stomatal anatomy and hydraulic traits. Smaller, denser stomata was correlated with faster stomatal closure at high VPD across the species of Rhizophoraceae, and stomata size negatively and vein density positively correlated with genome size. Less negative leaf osmotic pressure at the full turgor (π_o) was related to higher operating steady-state stomatal conductance (g_s); and a higher leaf capacitance (C_{leaf}) and more embolism resistant leaf xylem were associated with slower stomatal responses to an increase in VPD. In addition, stomatal responsiveness to VPD was indirectly affected by leaf morphological traits, which were affected by site salinity and consequently leaf water status. Our results demonstrate that mangroves display a unique relationship between genome size, stomatal size and vein packing, and that stomatal responsiveness to VPD is regulated by leaf hydraulic traits and stomatal morphology. Our work provides a quantitative framework to better understand of stomatal regulation in mangroves in an environment with high salinity and dynamic water availability.

1. Introduction

Stomata on the leaves of vascular plants dynamically control transpirational water loss (Meinzer, 1993). Under sufficient soil moisture and saturating light, stomatal conductance to water vapour (g_s) is mainly regulated by vapor pressure difference between leaves and the atmosphere (VPD). Stomata open to maximal extent at a low VPD in the morning, achieving the highest rate of carbon assimilation at this time. Once VPD begins to increase as the

* Corresponding author. State Key Laboratory for Conservation and Utilization of Subtropical Agro-Bioresources, College of Forestry, Guangxi University, Nanning 530004, China.
E-mail address: kunfangcao@gxu.edu.cn (K.-F. Cao).
Peer review under responsibility of Editorial Office of Plant Diversity.

https://doi.org/10.1016/j.pld.2024.02.003

day progresses stomata tend to close, reducing water potential decline to avoid a critical water tension that would induce xylem embolism (Sperry, 2000; Choat et al., 2018; Durand et al., 2019). In angiosperms, after a sudden increase in VPD, stomata often open initially because of a passive contraction of the epidermal cells, termed "wrong-way response" (WWR); showing a period of wrong-way opening stomata, and then closing gradually and reaching a new final steady-state (Buckley, 2016). This stomatal closure after a wrong-way opening is believed to be driven by the hormone abscisic acid (ABA), which is synthesized in leaves when mesophyll cells approach turgor loss point (McAdam and Brodribb, 2016). Unlike in species of lycophyte, fern and conifer, in which the kinetics of stomatal responses to VPD can be readily predicted by a passive hydraulic model of stomatal regulation (McAdam and Brodribb, 2015), in angiosperms stomatal closure at high VPD is believed to be largely driven by an active metabolic signal such as ABA (Brodribb and McAdam, 2011). Stomatal kinetics from initial steady-state to final steady-state in response to environmental fluctuation influences the balance between carbon assimilation (A) and water loss, and for this reason differences in kinetics can be adaptively relevant (Buckley, 2016; Meinzer et al., 2017; Lawson and Vialet-Chabrand, 2019; Durand et al., 2019). A fast stomatal kinetics, by closely tracking environmental perturbation, could enable stomata to operate optimally (Drake et al., 2013; Meinzer et al., 2017). Moreover, fast stomatal closure restricts transpirational water consumption and prevents hydraulic failure during rapid changes to high atmospheric water deficit (Martin-StPaul et al., 2017; Rodriguez-Dominguez and Brodribb, 2020).

Firstly, the rapidity of the g_s response to an increase in VPD in angiosperms might arise mechanistically from stomatal morphology (e.g., stomatal size and density). Smaller stomata have faster kinetics and greater responses to change in light, owing to a greater guard cell membrane surface area to volume ratio, which facilitates more rapid ion exchange (Drake et al., 2013). This hypothesis has been supported by some studies (Drake et al., 2013; Raven, 2014; Durand et al., 2019), but has not yet reached consensus (Elliott-Kingston et al., 2016; McAusland et al., 2016; Lawson and Vialet-Chabrand, 2019). Moreover, it has been found that stomatal morphologies, such as stomatal size and density, are correlated with genome size in angiosperms (Beaulieu et al., 2008; Simonin and Roddy 2018). If stomatal morphology mechanistically influences stomatal movement, a key unanswered question is whether the genome size in seed plants influences stomatal responses to fluctuating environmental conditions through its influence on stomatal morphology?

Additionally, stomatal responses to temporal rise in VPD might be affected by the hydraulic feedbacks that depends on leaf hydraulic resistance and water status (Buckley, 2005, 2019). For a species being highly vulnerable to dehydration, leaf hydraulic conductance often declines rapidly between full turgor and turgor loss point, which can further drive stomatal closure as a consequence of decrease in leaf water potential (Ψ_{leaf}) during leaf dehydration (Brodribb et al., 2014; Skelton et al., 2018). By contrast, in some species the leaf hydraulic system has strong resistance to water stress, with leaf hydraulic conductance declining slowly between full turgor and turgor loss point, and thus delaying stomatal closure during leaf dehydration (Scoffoni et al., 2012, 2017; Skelton et al., 2017). Stomatal regulation is influenced also by leaf water content (WC_{leaf}) with changing in cell volume, and hence the cell turgor pressure (Trueba et al., 2019; Fu et al., 2019; Xiong and Nadal, 2020). Leaf capacitance (C_{leaf}) is considered a key trait of water storage capacity in leaves, alleviating against rapid fluctuation in water potential and being involved in desiccation avoidance (Xiong and Nadal, 2020). Stomatal closure may thus be delayed in plants with a high C_{leaf}. Except in ferns and lycophytes (Martins et al., 2016), the relationship between the speed of stomatal closure and C_{leaf} in seed plants has been rarely examined explicitly.

Mangrove plants live in intertidal coastal zones of the tropics and subtropics (Duke et al., 1998), which are associated with high salt concentration and hypoxia in the soil rhizosphere as well as high atmospheric evaporative demand (Reef and Lovelock, 2015). To adapt to such habitats, mangroves have developed efficient regulation of water consumption, high resistance to xylem embolism, high tolerance to desiccation and high leaf capacitance, and they have hydraulic redistribution from the foliage to the stem for preserving stem hydraulic function (Reef and Lovelock, 2015; Jiang et al., 2017, 2021, 2022; Aritsara et al., 2022; Beckett et al., 2024). Mangroves have longer guard cell length for a given stomatal density than other vascular plants (Agduma et al., 2022) and evolved decreased genome size in adaptation to the intertidal habitat (He et al., 2022). Mangroves are confronted with increasing challenges for survival under global climate change, for example, a massive mangrove mortality in northern Australia occurred due to a severe El Niño event associated drought (Gauthey et al., 2022). Climate change will result in dramatic increase in VPD in tropical and subtropical regions. Yet, relatively little is known about the stomatal dynamics of mangroves in response to high VPD. In this study, we quantified the speed of stomatal closure in response to a step-rise in VPD *in situ*, and measured stomatal morphological characteristics, pressure–volume curves and hydraulic vulnerability to dehydration of leaves in nine true mangrove tree species. We aimed to answer the following two questions: (1) Does stomatal morphology influence stomatal dynamics in response to a high VPD in mangroves? with a consideration of possible influence of genome size on stomatal morphology; and (2) Do leaf hydraulic traits influence stomatal sensitivity to VPD in mangroves?

2. Materials and methods

2.1. Study site and plant material

The study sites were located at the Dongzhaigang Harbor National Nature Reserve in Hainan (19°57′ N, 110°35′ E), which has the largest mangrove forest area in China, and the Qinglangang Harbor Provincial Nature Reserve in Hainan (19°37′ N, 110°50′ E), which has the highest richness of mangrove species in China, respectively (Fig. 1). The two mangrove reserves are about 55 km apart and have similar climates, classified as a maritime monsoonal tropical climate. Mean annual temperatures are 23.8 °C (Jiang, 2021) and 23.9 °C (Leng, 2020) for the two sites, respectively; mean annual precipitation is about 1700 mm (Leng, 2020; Jiang, 2021), which is largely concentrated from May to November (Leng, 2020; Jiang, 2021); mean annual evaporation is about 1800 mm (Han, 2011; Leng, 2020); mean annual relative humidity is 85% (Han, 2011) and 87% (Leng, 2020), respectively. The soil types are mainly sandy saline soil and marsh saline soil; the salinity and water potential of soil is 5.71 g kg^{-1} and -1.88 MPa in Dongzhaigang, respectively, and 4.85 g kg^{-1} and -1.14 MPa in Qinglangan (Table 1). The salinity and water potential of tide is 23.84 g L^{-1} and -1.72 MPa in Dongzhaigang, respectively, and 10.06 g L^{-1} and -0.84 MPa in Qinglangan (Table 1).

Five mangrove species were selected in Dongzhaigang, including *Aegiceras corniculatum* (Myrsinaceae), *Avicennia marina* (Verbenaceae), *Ceriops tagal* (Rhizophoraceae), *Kandelia obovata* (Rhizophoraceae), and *Rhizophora stylosa* (Rhizophoraceae). Four mangrove species were selected in Qinglangang, including *Bruguiera gymnorhiza* (Rhizophoraceae), *B. sexangula* (Rhizophoraceae), *Sonneratia alba* (Sonneratiaceae), and *Xylocarpus granatum* (Meliaceae). These species are from five different families, all true mangrove species and the dominant or common species in the

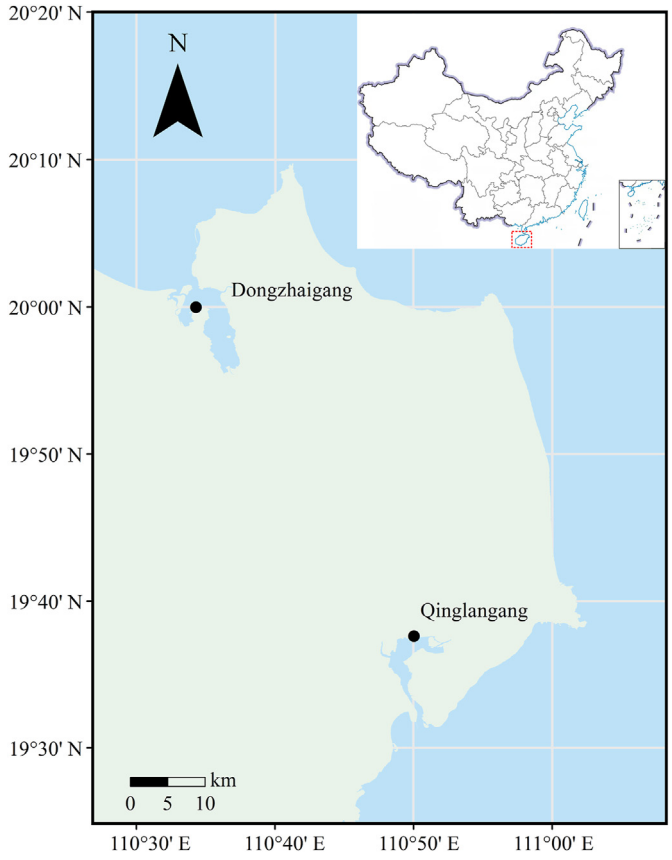

Fig. 1. The locations of the study sites. The red dashed rectangle in the inset marks Hainan Province, China. The black dots represent two coastal field sampling sites in Dongzhaigang and Qinglangang, Hainan Province, China. The salt concentrations and water potential of soil and tide at the two coastal field sites are shown in Table 1.

communities. They vary considerably in leaf hypodermal layers and stomatal morphology (Chen, 2020), and thus we would expect to find a diversity of stomatal regulation strategies across these species. Three to six mature, healthy and sun-exposed individuals of each species were selected for the experimental measurements. The information about height, basal diameter (BD), and the number of cell layers of the leaf hypodermis of the sampled plants are shown in Table 2.

2.2. Kinetics of stomatal response to temporal rise in VPD

Three to six, fully expanded and sun-exposed leaves of each species from different individuals in the field were selected for gas exchange measurement using a portable photosynthesis system (Li–Cor 6800; Li–Cor Inc.) on a clear day between 08:00 and 11:00 h (local time) from August to November 2020. Leaves were acclimatized inside the leaf cuvette (Photosynthetic Active Radiation, PAR, 1600 μmol m^{-2} s^{-1}; CO_2 concentration, 400 ppm; relative humidity, RH, 70%; flow rate, 500 μmol s^{-1}) until stomatal conductance (g_s) reached an initial steady-state ($SS_{initial}$; defined as a variation < 5% over 3 min), during which the leaf chamber temperature were controlled to 0–2 °C below the air temperature. At this point, RH was then switched to 20%, resulting in a step-increase in VPD while no change in other environmental parameters, and g_s showed a transient increase for about 3 min, called the "wrong-way response" (WWR), then declined gradually until it reached a new final steady-state (SS_{final}). The VPD was about 0.95 kPa and 2.65 kPa before and after changing RH, respectively (Fig. S1). The value of g_s was recorded every 20 s during the entire measurement period. After the measurements of gas exchange, the intact branches from which the leaves grew were marked for subsequent measurements of pressure–volume curves and hydraulic vulnerability to dehydration of leaves.

2.3. Leaf predawn and midday water potential

On the day of measuring gas exchange, leaf predawn water potential (Ψ_{pd}) and midday water potential (Ψ_{md}) were measured using a pressure chamber (PMS Instruments) between 4:30 to 6:30 h, and 12:30 to 14:30 h, respectively. For measuring Ψ_{pd}, two leaves from four-five individuals per species were wrapped up with aluminium foil and plastic bags on the previous evening of gas exchange measurements. For measuring Ψ_{md}, two leaves from the same individual as the leaves used for Ψ_{pd} measurements were excised, and then immediately enclosed in aluminium foil and plastic bags. All measurements were made in the field within 10 min after excision.

2.4. Pressure–volume curves

Pressure–volume measurements were performed on leaves using the bench drying procedures described by Tyree and Hammel (1972). A branch neighboring those measured for gas exchange was harvested for each species and rehydrated overnight for next-day measuring from August to November 2020. One fully expanded leaf was collected from each rehydrated branch and dehydrated on the bench in a temperature-controlled room with a good-ventilation. The leaf was repetitively weighted and measured for water potential with a pressure chamber (PMS Instruments). The early and late interval time of each curve measurement was 0.5–2 h and 4–8 h, respectively. Determining a complete pressure–volume curve with least 10 points required leaves to dehydrate for 2–4 days. Furthermore, leaf area was analysed using a scanner and dry mass was determined after oven-drying for 72 h at 60 °C. From three to six pressure–volume curves for each species (Fig. S4), the following parameters were determined as in Sack and Pasquet-Kok (2011): osmotic potential at full turgor (π_o) and at turgor loss point (π_{tlp}), bulk modulus of elasticity (ε) and leaf area specific capacitance at full turgor (C_{leaf}) (Table S1).

Table 1
Physicochemical properties of soil and tide in two sites. Values are means ± SE (n = 5). An independent-samples *t*-test was used to compare the differences in salinity and water potential of soil and tide between the two sites.

	Parameter	Symbol	Dongzhaigang	Qinglangang	*t*-Test
Soil	Salinity	SAL_{soil}	5.71 ± 0.64 g kg^{-1}	4.85 ± 0.51 g kg^{-1}	$p < 0.05$
	Water potential	Ψ_{soil}	-1.88 ± 0.11 MPa	-1.14 ± 0.1 MPa	$p < 0.001$
Tide	Salinity	SAL_{tide}	23.84 ± 1.46 g L^{-1}	10.06 ± 0.54 g L^{-1}	$p < 0.001$
	Water potential	Ψ_{tide}	-1.72 ± 0.03 MPa	-0.84 ± 0.05 MPa	$p < 0.001$

Note: Soil samples were collected at low tide. Tide samples were collected at high tide. The salinity was measured by weight method (Bao, 2000). The water potential was measured using a dew point water potential instrument (WP4C, Decagon Devices, Pullman, WA, USA).

Table 2
The basic information for the sample plants of nine mangrove species studied in two sites. *Avicennia marina* only has hypodermal layers beneath the upper epidermis (marked with an asterisk), *Sonneratia alba* has no hypodermal layers, the rest species have hypodermal layers beneath both upper and lower epidermises. Values are means (minimum, maximum) for height, BD, basal diameter or means ± SE for leaf predawn water potential (Ψ_{pd}) and leaf midday water potential (Ψ_{md}).

Species (*Abbr.*)	Family	Mean Height (range) (m)	Mean BD (range) (cm)	Number of Hypodermis	Ψ_{pd} (-MPa) means ± SE	Ψ_{md} (-MPa) means ± SE	site
Aegiceras corniculatum (AC)	Myrsinaceae	2.1 (1.8, 2.4)	4.8 (4, 6)	4–6	1.71 ± 0.18	2.97 ± 0.14	Dongzhaigang
Avicennia marina (AM)	Verbenaceae	2.8 (2.6, 3)	7.2 (6.7, 8.2)	6-8*	2.57 ± 0.19	4.39 ± 0.18	Dongzhaigang
Ceriops tagal (CT)	Rhizophoraceae	2.3 (2.1, 2.5)	9.2 (7.5, 11.8)	3–4	2.59 ± 0.1	3.17 ± 0.12	Dongzhaigang
Kandelia obovata (KO)	Rhizophoraceae	3.7 (3.2, 4.1)	10.3 (8, 14)	4	2.17 ± 0.08	3.47 ± 0.14	Dongzhaigang
Rhizophora stylosa (RS)	Rhizophoraceae	4 (3.6, 4.4)	7.6 (6.7, 9.5)	6–9	2.27 ± 0.14	3.06 ± 0.19	Dongzhaigang
Bruguiera sexangular (BS)	Rhizophoraceae	5.8 (4.4, 7)	18.9 (10, 29)	2	1.77 ± 0.1	2.54 ± 0.29	Qinglangang
Bruguiera gymnorhiza (BG)	Rhizophoraceae	4.7 (4, 6.8)	18.1 (11.5, 22.4)	2	1.9 ± 0.12	2.53 ± 0.19	Qinglangang
Sonneratia alba (SA)	Sonneratiaceae	8 (6.5, 8.9)	22.66 (14, 33.4)	0	1.91 ± 0.14	2.5 ± 0.17	Qinglangang
Xylocarpus granatum (XG)	Meliaceae	4.7 (4, 5.5)	18.76 (11, 27.5)	3–5	1.71 ± 0.16	2.8 ± 0.18	Qinglangang

2.5. Leaf hydraulic vulnerability curves

Branches from three to six individuals, approximately 110 cm in length that at least twice the maximum vessel length of these species (Jiang, 2021), neighboring those measured for gas exchange for each species were collected and recut immediately under water in May to June 2021. Furthermore, the cut ends of the branches were wrapped in damp towels, which were wrapped tightly by tiny plastic bags with some amount of water in it. Then, the branches were quickly placed in black plastic bags and brought back to the laboratory. All branches were recut underwater again, sealed with in black plastic bags, and allowed to rehydrate overnight in the laboratory. The cut ends of branches were wrapped by wax and parafilm (PM996; BEMIS). Leaf vulnerability curves were obtained using the rehydration method described by Brodribb and Holbrook (2003). According to the leaf vulnerability curve with least 60 points for each species (Fig. S5), we determined the maximum hydraulic leaf conductance (K_{leaf}), the water potentials inducing 12% (P_{12}) and 50% (P_{50}) loss of the maximum conductance (Table S1).

2.6. Modelling g_s responses to a step-rise in VPD

Stomatal temporal dynamics in response to a single step-rise in VPD was fitted empirically using an analytical sigmoidal model (Vialet-Chabrand et al., 2013) to evaluate the specific parameters in the response curve of g_s (Fig. 2). It describes as (Eq. (1)):

$$g_s = g_{s-initial} + \left(g_{s-final} - g_{s-initial}\right) \cdot e^{-e^{[(\lambda - time)/\tau]}} \quad (1)$$

where g_s ($mol \cdot m^{-2} \cdot s^{-1}$) is the g_s at the corresponding time (s), λ the initial time lag of the sigmoidal curve (s), τ the time constant of g_s response (s), $g_{s\text{-initial}}$ and $g_{s\text{-final}}$ ($mol \cdot m^{-2} \cdot s^{-1}$) are the steady-state values of g_s at the initial and final stages of a sigmoidal curve, respectively. *e* is Euler's number (c. 2.718). Based on these parameters, we obtained the second parameter, the maximum slope (SL_{max}) ($mmol \cdot m^{-2} \cdot s^{-1}$) (Eq. (2)) as an estimator of combining speed and amplitude of the g_s response to the step-rise in VPD:

$$SL_{max} = \frac{g_{s-final} - g_{s-initial}}{\tau \times e} \quad (2)$$

More details on the model and its parameters can be referred to the literature (Vialet-Chabrand et al., 2013; Durand et al., 2019).

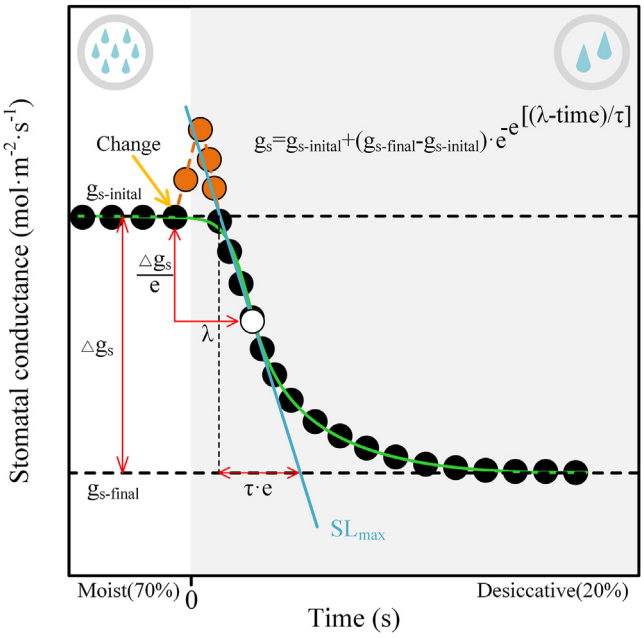

Fig. 2. Summary of the parameters derived from a sigmoidal model of changes in stomatal conductance (g_s) in response to a step-rising of vapour pressure deficit (VPD). The yellow arrow showed the time at which VPD was increased. $g_{s\text{-initial}}$ and $g_{s\text{-final}}$ are the stomatal conductance values at the initial and the final steps of the curve, respectively. Δg_s is the magnitude of changes in g_s ($\Delta g_s = g_{s\text{-initial}} - g_{s\text{-final}}$). λ is the time between the VPD change and the moment where the change of g_s is at a maximum (white dot). SL_{max} is the tangent (blue line) that goes through this point of the maximum speed of the stomatal response and is determined as $\Delta g_s/(\tau \cdot e)$ where $e \approx 2.718$. The orange points represent stomatal "wrong-way" response (WWR), which is a transient passive stomatal opening due to a rapid reduce in epidermal turgor and a less backpressure on the guard cells results from rising transpiration following elevating VPD. Our goal was to discuss the effect of hydraulic-related traits on stomatal VPD response time and thus curve-fitting (green line) did not include the data of WWR. The blank area indicates a moist status with relative air humidity of 70%, and while grey area indicates a desiccative status with relative air humidity of 20%.

2.7. Leaf morphology and stomatal anatomy

Leaves used for gas exchange measurements or in the neighboring were collected, enclosed in plastic bags, and immediately refrigerated at 4 °C. Each species had five leaves from different trees in total. Transverse cross-sections avoiding major veins were made with hands. All sections were stained with 1% Safranin-Alcian blue, washed with distilled water, and then mounted on microscope

slides. They were observed under a light microscope (Leica DM 3000 LED Wetzlar Germany), and imaged for measurement of tissue thickness. Paradermal sections were sliced from each leaf with a square puncher (~1 cm^2), avoiding major veins, and soaked overnight in a bleach solution composed of hydrogen peroxide and acetic acid (H_2O_2:CH_2COOH = 1:1) at 70 °C in an oven. For the measurement of leaf vein density, transparent paradermal sections were stained with 0.5% safranin, washed with distilled water, and then mounted on microscope slides. They were observed under the light microscope, capturing five images per leaf at magnifications of 5× for vein length measurements. For the measurement of stomatal traits, transparent epidermal samples were isolated from the mesophyll and washed with distilled water. These samples were stained with 1% Safranin-Alcian blue, washed with distilled water, and then mounted on microscope slides. They were observed under the light microscope, capturing five images per leaf at magnifications of 10× for stomatal density and 40× for stomatal size measurements. ImageJ software was used to measure leaf thickness (LT), hypodermis thickness (HT), vein length, stomatal number and guard cell length (*GCL*). The fraction of hypodermis to lamina thickness ($HT_{fraction}$) was calculated as $HT_{fraction}$ = HT/LT. Stomatal density (*SD*) was the number of stomata per mm^2. Leaf vein density (VD) was calculated as the total length of veins per mm^2. Anatomical maximum stomatal conductance ($G_{s\text{-}max}$) was calculated according to the method described by de Boer et al. (2016b). Stomatal opening ratio at the initial steady-state ($G_{s\text{-}ratio}$) was calculated as $G_{s\text{-}ratio} = g_{s\text{-}initial}/G_{s\text{-}max}$.

2.8. Statistics and graphics

Genome sizes of nine mangrove species were collected from the two literatures, He et al., (2022); Hu et al., (2020), and were shown in Table S1. Remarkably, mangroves have a smaller genome assembly compared to other angiosperms (Jiang et al., 2023).

An independent-samples *t*-test was used to compare the differences in salinity and water potential of soil and tide between the two sites. Stomatal dynamics was fitted using a sigmoidal model in SigmaPlot 12.5, excluding stomatal transient WWR. The leaf vulnerability curves were fitted in SigmaPlot 12.5. Linear regression analyses were performed using species' average values to examine the interspecific relationship between leaf water transport efficiency, gas exchange and water relations in nine mangrove species. Correlations were computed using mean values by performing linear regression analyses with stomatal dynamics parameters as dependent variables and stomatal morphology, total assembled genome size, leaf osmotic pressure, leaf dehydration tolerance, leaf predawn water potential or leaf capacitance as continuous independent variables across the nine mangrove species. The correlations were considered statistically significant if $p < 0.05$. All regression analyses, figures and *t*-tests were made using the R-project v.4.1.1 (https://www.r-project.org/).

Partial Least Squares Path Modeling (PLS-PM) was used to build the network of relationships between the measured variables through latent variables for exploring the cause-and-effect link between environmental factors of the sites, leaf water status, leaf morphology, hydraulic traits, stomatal anatomy and stomatal dynamics. The conceptual framework among latent variables was established based on known relationships and previous understandings of environmental factors of the sites, leaf water status, leaf hydraulic traits, stomatal anatomy and stomatal dynamics. In this framework, the environmental factors of the sites were presented by Ψ_{soil}, Ψ_{tide} SAL_{soil} and SAL_{tide}. Leaf water status was described by Ψ_{pd} and Ψ_{md}. Leaf morphology was described by LMA, VD, LT, HT, $HT_{fraction}$. Stomatal anatomy was presented by *SD*, *GCL*, $G_{s\text{-}max}$ and $G_{s\text{-}ratio}$. Hydraulic trait was presented by C_{leaf}, K_{leaf}, π_0, P_{12} and P_{50}. Stomatal dynamics was determined by $g_{s\text{-}initial}$, $g_{s\text{-}final}$, Δg_s, λ, τ and SL_{max}. PLS-PM were run in the R-project v.4.1.1 (https://www.r-project.org/) using packages "plspm", and performed with 1000 bootstraps to obtain path coefficients and R^2 values for each latent variable and its statistical significance and standardized loading values of each measured variable to its latent variable and Goodness-of-Fit index of the path models.

3. Results

3.1. Correlations between stomatal dynamics, stomatal morphology, vein network and genome size

The nine mangrove species varied considerably in stomatal size and stomatal density (*SD*) (Fig. 3). Guard cell length (*GCL*) varied from 23.68 to 45.84 μm, and *SD* from 123.62 to 386.64 no·mm^{-2}. By the bivariate trait-relationship analysis, these stomatal morphological properties were not related to the speed of stomatal responses to a step-rise in VPD across all species from five families (Fig. 3). But for the five mangrove species of Rhizophoraceae, the stomatal response time constant (τ) was positively correlated with *GCL* ($R^2 = 0.773$; Fig. 3a) and negatively with *SD* ($R^2 = 0.78$; Fig. 3b); and the maximum speed of stomatal closing (SL_{max}) also showed a positive relationship with *SD* ($R^2 = 0.797$; Fig. 3c). However, in our path modeling, the variation in stomatal dynamics was affected directly by stomatal anatomy with the total effect of -0.64 (Fig. 7). These results indicate that stomatal behavior in response to a step-rise in VPD are regulated directly by stomatal anatomy, with smaller and more numerous stomata have faster kinetics than leaves with larger stomata, while across diverse mangrove genera there is no general relationship between stomatal anatomy and responsiveness.

Furthermore, genome size was significantly correlated negatively with *GCL* and positively with leaf vein density (VD) among the mangrove species excluding an outlier (Fig. 3d, f). However, genome size was not associated statistically with the speed of stomatal responses to a step-rise in VPD across all species, or even within Rhizophoraceae (Fig. S2). We also observed that *SD* was positively correlated with VD and the leaf osmotic potential at full turgor (π_o) (Figs. S3a–b), and the initial steady-state g_s ($g_{s\text{-}initial}$), the final steady-state g_s ($g_{s\text{-}final}$) and the amplitude of variation in g_s (Δg_s) in response to a step-increase in VPD were significantly and positively correlated with π_o among the mangrove species excluding an outlier (Fig. 4a–c). However, π_o was not statistically related to the parameters of stomatal dynamics in responses to a temporal rise in VPD across the nine mangrove species, even if excluding an outlier (Fig. 4d–f). $g_{s\text{-}initial}$ was significantly and positively correlated with the maximum leaf hydraulic conductance (K_{leaf}) among the mangrove species (Fig. S3c). These results indicate that operating steady-state g_s is related to leaf osmotic pressure and hydraulic conductance, which is closely linked to stomatal morphology and vein construction, controlled by genome size.

3.2. Stomatal dynamics in relation to leaf hydraulic traits

Firstly, the species with less negative P_{12} had a higher maximum stomatal response speed (SL_{max}) and faster the time constant (τ) and the lag time (λ) of g_s response during stomatal closing response to a step rising VPD (Fig. 5a–c), but the water potential inducing 50% loss of the leaf maximum conductance (P_{50}) was not statistically related to SL_{max}, τ, and λ (Fig. 5d–f), indicating that P_{12} and not P_{50}, might be critical for stomatal regulation and that a lower vulnerability of leaves to dehydration could lengthen stomatal closing time in response to a step-rising of VPD. Moreover, leaf

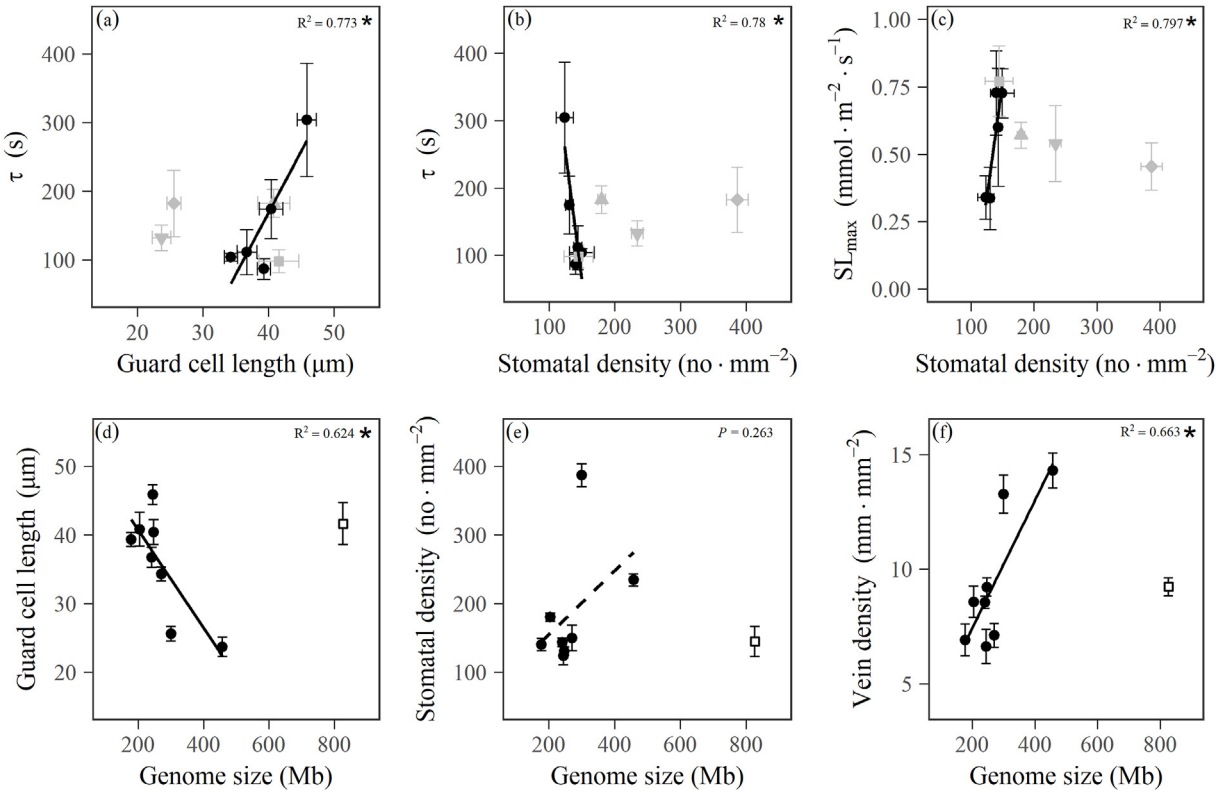

Fig. 3. Relationships between genome size, stomatal morphology and parameters describing the kinetics of stomatal closure in response to a step-rising of vapour pressure deficit (VPD), the genome size data are from He et al. (2022) and Hu et al. (2020). Correlations between the response time constant τ during stomatal closing response to a step rising VPD and guard cell length (a), or stomatal density (b) across five mangrove species of Rhizophoraceae, between the maximum speed of the stomatal VPD response at the inflection point of the curve (SL_{max}) and stomatal density (c) across the five mangrove species of Rhizophoraceae. Correlations between genome size and guard cell length (d), stomatal density (e), or leaf vein density (f). The significant relationships were fitted with lines among five mangrove species of Rhizophoraceae, which is indicated by black circles (a–c). Grey symbols denote for the other four mangrove species of different family, which were not included in the regression (a–c). White rectangles represent *Aegiceras corniculatum*, which was not included in the regression (d–f). Points and error bars represent means and the standard error (±SE) for each species, respectively. *$p < 0.05$.

capacitance (C_{leaf}) was positively and significantly correlated ($R^2 = 0.775$) with τ and was negatively correlated ($R^2 = 0.714$) with SL_{max} (Fig. 6a–b) among the mangrove species excluding a single outlier species (*Ceriops tagal*), indicating that under a high transpiration demand, high C_{leaf} could delay the stomatal closure. Moreover, the results of the path analysis reveal that the variations in stomatal dynamics were explained directly by leaf hydraulic traits with the total effect of 0.88 (Fig. 7), which reinforced our observation based on bivariate relationship stated above.

Additionally, the species with lower bulk modulus of elasticity (ε) had higher leaf capacitance (C_{leaf}) (Fig. S3d), which was related significantly to lamina hypodermis thickness (HT) and hypodermis fraction ($HT_{fraction}$) (Figs. S3e–f). These results indicate that leaf structural traits that are associated with water storage, especially in the hypodermis, have indirect effects on stomatal dynamics through the influence on hydraulic traits (Fig. 7). Leaf water status, which was proportional to site salinity, had also indirect impacts on stomatal dynamics by changing in hydraulic traits (Fig. 7), as that species with more negative P_{12} and P_{50} had a more negative leaf predawn water potential (Ψ_{pd}), and the latter was negatively correlated with λ (Fig. 5g–i).

4. Discussion

We found evidence that the morphology of stomata and hydraulic traits of leaves influences stomatal response to a step-increase in VPD in mangrove trees. Rhizophoraceae species (but not all mangrove species) with smaller and denser stomata had faster stomatal responses to the step-rise of VPD. Across all species those with higher vulnerability to initial loss of hydraulic conductance during dehydration had faster stomatal responses and the opposite was true for the species with higher leaf capacitance. In addition, partial least squares path modeling showed that the water potential and salinity of the sites determined leaf water status of mangroves. They in turn influenced leaf morphology, which indirectly affected on stomatal dynamics through the variations in both stomatal anatomy and hydraulic traits in mangroves. These regulatory behaviors of stomata could be of vital importance for the long-term survival of mangrove trees in a stressful environment.

4.1. A key role of stomatal morphology in stomatal dynamics

Smaller stomata have often considered to have faster kinetics (Drake et al., 2013). In the present study, we observed a trend of increasing speed of stomatal closure with increasing stomatal density (*SD*) and decreasing guard cell length (*GCL*) in the five mangrove species of Rhizophoraceae, but this pattern was not found across all nine mangrove species from different families. Elliott-Kingston et al. (2016) found no relationship between stomatal closure rapidity and size or density of stomata in an evolutionary diverse series of species (including fern, cycad, conifers and angiosperms). Likewise, McAusland et al. (2016) examined rapidity of stomatal closure from species over a range of crops with differences in stomatal morphology (kidney- or elliptical-shaped) and found that stomatal kinetics was also not explained by the size of stomata. Overall, our study is generally consistent with previous

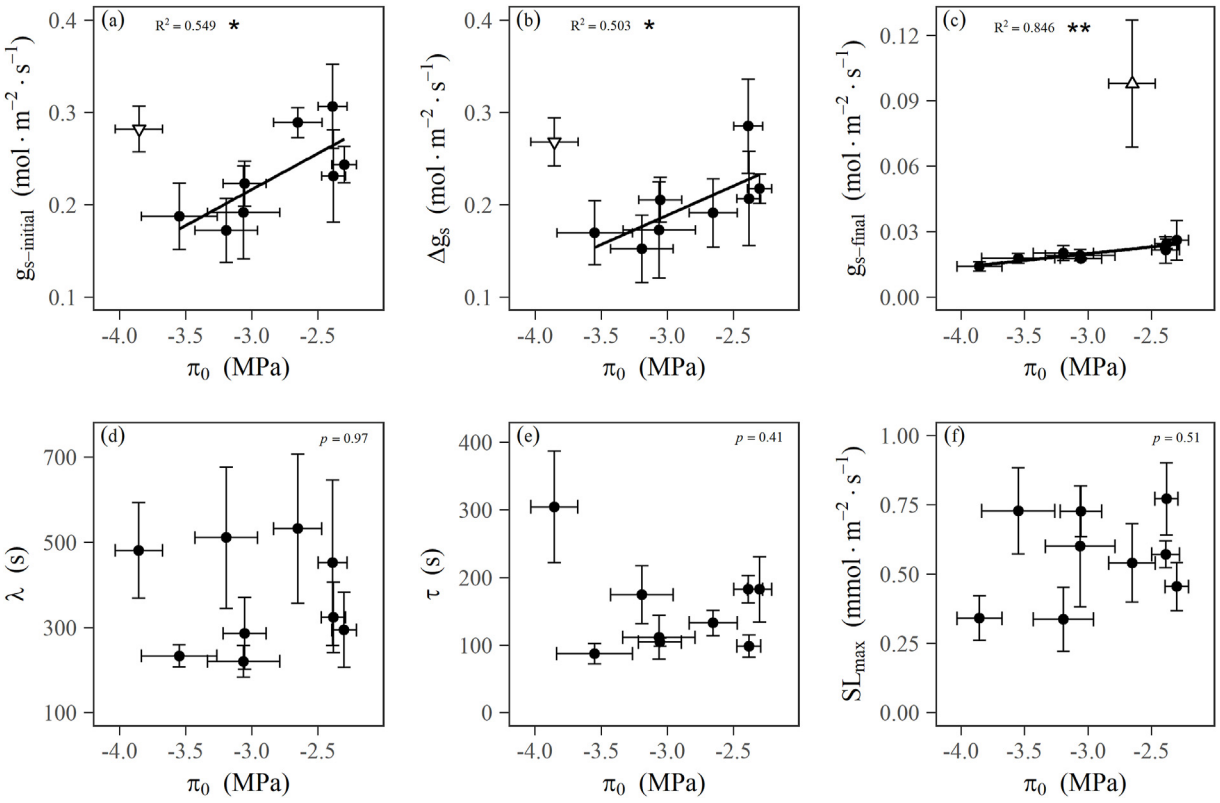

Fig. 4. Relationships between gas exchange and leaf osmotic pressure. Correlations between the leaf osmotic potential at full turgor (π_o) and the steady-state values of g_s at the initial step of the curve ($g_{s\text{-initial}}$) (a), the amplitude of variation in g_s during an increase in VPD (Δg_s) (b), the steady-state values of g_s at the final step of the curve ($g_{s\text{-final}}$) (c), the lag time λ for stomatal closing as a response to VPD (d), the response time constant τ during stomatal closing response to a step rising VPD (e), or the maximum speed SL_{max} of the stomatal VPD response at the inflection point of the curve (f), across mangrove species, respectively. The regression lines were fitted for the significant relationships, excluding outliers indicated by white inverted triangles (a–b) and white triangle (c) for *Ceriops tagal* and *Avicennia marina*, respectively; because there might be distinctive strategies in adaptation to atmospheric drought for *C. tagal* with the most negative π_{tlp} (most negative value), showed an extremely strong the ability of maintaining leaf osmotic pressure, which was able to maintain a relatively constant osmotic potential over a large range in relative water contents, and *A. marina* with a trichome layer covering stomata on the abaxial leaf surface, which can effectively reduce transpirational water loss within the vicinity of the stomatal pore (peristomatal) by increasing the boundary-layer resistance to vapor diffusion. Points and error bars represent means and the standard error (±SE) for each species. *$p < 0.05$; **$p < 0.01$.

studies and suggests that the relationship between stomatal closing speed in response to a step-rise in VPD and stomata size is conserved in closely related species, but not across lineages. There may be mechanisms that affect stomatal movement speed in response to ambient environmental fluctuation independent of stomatal size across species with diverse stomata morphology. As shown by the present study that stomatal behavior was strongly regulated by hydraulics (e.g., the water potential inducing 12% loss of leaf hydraulic conductance, P_{12}) and water-relations traits of leaves (discussed below).

We also observed that operating steady-state g_s in responses to a step-increase in VPD were determined by leaf osmotic adjustment, and that species with a higher *SD* had a less negative bulk leaf osmotic potential at full turgor (π_o). The positively relationship between *SD* and π_o would likely constrain stomatal behavior in response to high atmospheric water deficit. These findings are consistent with the recent proposal that species with less negative π_o and osmotic potential at turgor loss point (π_{tlp}) had smaller, denser stomata and higher maximum operating steady-state g_s and greater sensitivity in stomatal closure during leaf dehydration over a wide range of species (Henry et al., 2019). Our work on the nine mangrove species, which have more negative π_o and π_{tlp} than most of terrestrial plants, provides an important support for the idea of stomatal safety-efficiency trade-off (Henry et al., 2019). However, leaf osmotic pressure was not correlated with stomatal dynamics in responses to a temporal rise in VPD across the nine mangrove species in this study. The stomatal response to a high VPD might involve in the dynamics of synthesis and breakdown of some biochemical materials (e.g., abscisic acid and protein kinases) (McAdam and Brodribb, 2015; Jalakas et al., 2021).

Our results also showed that genome size was correlated significantly and negatively with guard cell length (*GCL*), and positively with vein density (VD) among mangrove species excluding an outlier. It must be noted that the inverse relationship of genome size and stomatal size across the mangrove species is not in conflict with previous studies (Beaulieu et al., 2008). The universal relationship between genome size and *GCL* is found at large-scale comparative analyses over a wide range of species (Beaulieu et al., 2008), while the negative relationship in mangroves of our study was shown by a little variation in genome size at small-scale from nine species. This finding is consistent with recent work on genome size, leaf cell size and cell packing density relationships in a range of mangroves (Jiang et al., 2023). Nevertheless, genome size showed nonsignificant association with the rapidity of stomatal closure response to an increase in VPD among the nine mangrove species. Compared to other angiosperms, mangroves had a smaller genome (Jiang et al., 2023), a faster VPD response (Fig. S6), and a larger *GCL* and higher vein density at a given *SD* (Agduma et al., 2022). Therefore, mangroves adapted to the stressful intertidal habitat may change the genome size-stomatal dynamics relationship for optimal water use.

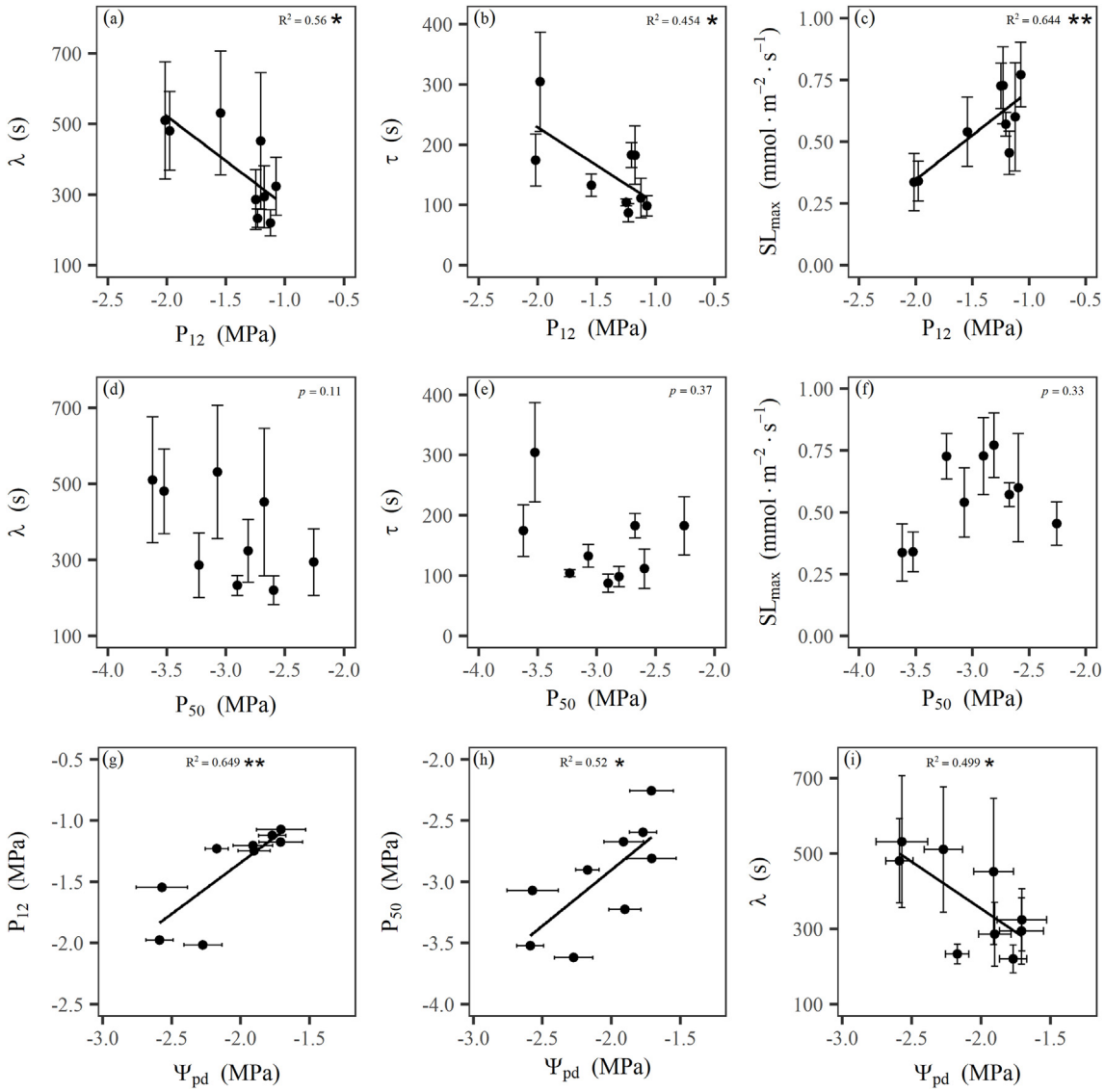

Fig. 5. Relationships between leaf hydraulic traits and parameters describing the kinetics of stomatal closure in response to a step-rising of vapour pressure deficit (VPD) across the mangrove species. Correlations between the water potential inducing 12% (P_{12}) loss of the maximum conductance of leaves and the lag time λ for stomatal closing as a response to high VPD (a), the response time constant τ during stomatal closing response to a step increase in VPD (b) and the maximum speed (SL_{max}) of the stomatal response to high VPD at the inflection point of the curve (c), respectively. Correlations between P_{50} and λ (d), τ (e), or SL_{max} (f), respectively. Correlations between leaf predawn water potential (Ψ_{pd}) and P_{12} (g), P_{50} (h), or λ (i), respectively. Points and error bars represent means and the standard error (±SE) for each species, respectively. *$p < 0.05$; **$p < 0.01$.

4.2. Leaf hydraulic vulnerability and capacitance affect stomatal regulation behavior

Our results showed that the water potential inducing 12% loss of the maximum conductance of leaves (P_{12}) is a strong regulator of the kinetics of stomatal closure in response to a temporal rise in VPD in the mangroves. Firstly, P_{12}, which is the initial inflection point of the vulnerability of leaf hydraulic conductance to dehydration, is considered as a potential trigger for stomatal closure as explained by simple hydraulic feedback (Buckley and Mott, 2002; Buckley, 2005). Secondly, P_{12} reflects the primary hydraulic resistance to bulk flow of the liquid-phase moving from xylem into the bundle sheath to epidermal cells and guard cells within leaves during dehydration (Sack and Holbrook, 2006). It may drive an initial increase in the opposing effect of the epidermal pavement cells on guard cells (Darwin, 1898; Cowan, 1977), triggering hydraulic feedback for stomatal closure (Buckley, 2019). Lastly, the whole-leaf hydraulic resistance also includes the vapour-phase diffusion from the evaporating sites to stomata (Buckley et al., 2017), which is linked with the liquid transport in transpiring leaves and closely related to water potential (Rockwell et al., 2014). It, therefore, is likely that species with more negative P_{12} have faster vapour diffusion through stomata (Peak and Mott, 2011), which would delay stomatal closure in response to atmospheric drought. However, the water potential corresponding to 50% loss in leaf hydraulic conductance (P_{50}) was not significantly correlated with the kinetics of stomatal closure in response to a step-rise in VPD across the mangrove species. The adaptation of P_{12}, not P_{50}, as a strong linker of kinetics of stomatal closure in response to a step-rise in VPD may contribute to the trigger of hydraulic feedbacks and translate this message into next effector that participates in the dynamic behavior of stomata (Tardieu, 2016; Choat et al., 2018). This initial hydraulic P_{12} message drives fast stomatal closure in response to a step rise VPD to limit transpiration and timely

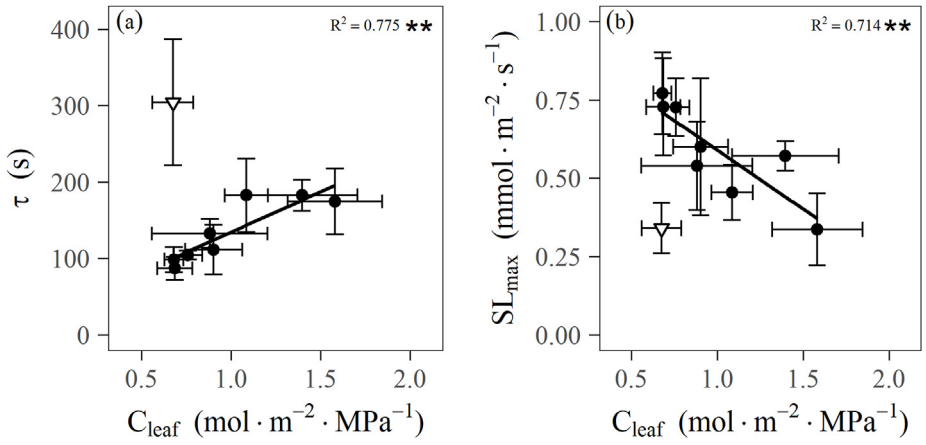

Fig. 6. Relationships between leaf capacitance (C_{leaf}) and parameters describing the kinetics of stomatal closure in response to a step-rising of vapour pressure deficit (VPD) across the mangrove species: the response time constant τ during stomatal closing response to a step-rise in VPD (a), and the maximum speed (SL_{max}) of the stomatal response at the inflection point of the curve (b). White inverted triangle (a–b) is for *Ceriops tagal* with the most negative π_{tlp}, showed an extremely strong the ability of maintaining leaf osmotic pressure, which was able to maintain a relatively constant osmotic potential over a large range in relative water contents and could be distinguished from the nine mangrove species; it thus was excluded in the correlations. Points and error bars represent means and the standard error (±SE) for each species, respectively. $^{**}p < 0.01$.

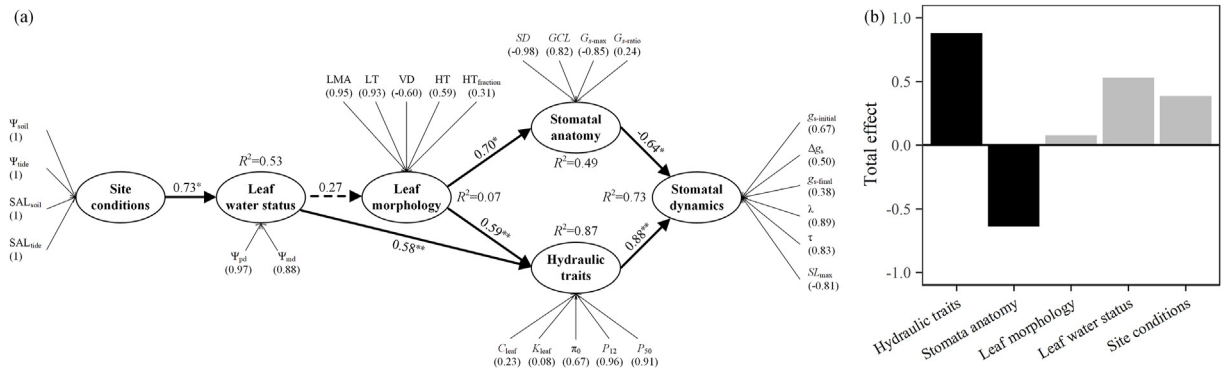

Fig. 7. The graph of the Partial Least Squares Path Model (PLS-PM) results, illustrating the relationships between stomatal dynamics ($g_{s\text{-}initial}$, $g_{s\text{-}final}$, Δg_s, λ, τ, SL_{max}), stomatal anatomy (*SD*, *GCL*, $G_{s\text{-}max}$, $G_{s\text{-}ratio}$), hydraulic traits (C_{leaf}, K_{leaf}, π_0, P_{12}, P_{50}) leaf morphology (LMA, LT, VD, HT, $HT_{fraction}$), leaf water status (Ψ_{pd}, Ψ_{md}), the water potential and salinity of the sites (Ψ_{soil}, Ψ_{tide}, SAL_{soil}, SAL_{tide}). The PLS-PM explained 73% of the variations in stomatal dynamics across the mangrove species. (a) Traits within the ellipses are latent variables, which are presented by measured variables outside the ellipses. The values in parentheses represent the loadings of measured variables to its latent variable. The solid and dotted arrows represent the significant and nonsignificant relationships between two latent variables, respectively. The measured variables were standardized to use in the path model. The (−) and (+) numbers adjacent to arrows represent the negative and positive relationships by standardized path coefficients, respectively. $^{*}p < 0.05$; $^{**}p < 0.01$. R^2 represents the proportion of variance explained by the model. The Goodness of Fit index of the model was 0.57. (b) The total effects of these latent variables on stomatal dynamics. The variations in stomatal dynamics were affected directly by stomatal anatomy and were affected directly by leaf hydraulic traits, and with the total effect of -0.64 and 0.88, respectively. Leaf morphology exhibited indirect effects on stomatal dynamics through the variations in both stomatal anatomy and hydraulic traits with the total effect of 0.08. Leaf water status had also indirect impacts on stomatal dynamics by changing in hydraulic traits with the total effect of 0.53. The total effect of the salinity of soil and tide of the sites on stomatal dynamics were 0.39, which was principally contributed by the influence of leaf water status on hydraulic traits. Ψ_{soil}: the water potential of soil; Ψ_{tide}: the water potential of tide; SAL_{soil}: the salinity of soil; SAL_{tide}: the salinity of tide; Ψ_{pd}: leaf predawn water potential; Ψ_{md}: leaf midday water potential; LMA: leaf mass per area; LT: leaf thickness; VD: vein density; HT: hypodermis thickness; $HT_{fraction}$: the fraction of hypodermis to lamina thickness; *SD*: stomatal density; *GCL*: guard cell length; $G_{s\text{-}max}$: the anatomical maximum stomatal conductance; $G_{s\text{-}ratio}$: stomatal opening ratio at the initial steady-state; C_{leaf}: leaf capacitance; K_{leaf}: the maximum leaf hydraulic conductance; π_o: leaf osmotic potential at full turgor; P_{12}: the water potentials inducing 12% loss of the maximum leaf hydraulic conductance; P_{50}: the water potentials inducing 50% loss of the maximum leaf hydraulic conductance; $g_{s\text{-}initial}$: the steady-state values of g_s at the initial step of the curve; $g_{s\text{-}final}$: the steady-state values of g_s at the final step of the curve; Δg_s: the amplitude of variation in g_s during an increase in VPD; λ: the lag time for stomatal closing as a response to VPD; τ: the response time constant during stomatal closing response to a step rising VPD; SL_{max}: the maximum speed of the stomatal closing response to a step rising VPD at the inflection point of the curve.

prevent a dramatic decline in leaf water potential (Buckley, 2019), and thus is of crucial importance for the long-term survival of mangrove trees.

Additionally, we observed that mangroves developed thick or even upper and lower hypodermis, contributing a large proportion of lamina thickness and storing a considerable amount of water inside leaves, thus had high leaf capacitance (C_{leaf}). Leaves with a high C_{leaf} can buffer fluctuation in leaf water potentials when facing atmospheric drought, by compensating transpirational water loss from storage water. Therefore, we observed a significant trend of increasing time of stomatal closure in response to a step-rise in VPD in the mangrove species with higher C_{leaf}. This is consistent with previous studies (Martins et al., 2016; Fu et al., 2019; Xiong and Nadal, 2020). Although the high C_{leaf} of the mangroves may delay stomatal closure at high VPD, the mangrove species with a high C_{leaf} had a faster stomatal VPD response than the six glycophytic woody species measured by Fu et al. (2019) (Fig. S6). Thin leaves of these glycophytic species could systematically alleviate the instantaneous decline of leaf water potential under an atmospheric drought due to a shorter hydraulic pathway from vascular bundle to stomata so that generate a smaller water potential gradient across mesophyll tissues (Brodribb et al., 2007; de Boer et al., 2016a; Buckley

et al., 2017) and thus slower stomatal VPD response, because water potential would not drop close to π_{tlp} when abscisic acid (ABA) would be synthesized in leaves (McAdam and Brodribb, 2016). By contrast, the thick leaves of mangrove trees with longer outside-xylem pathways of water transport are difficult to maintain water balance between mesophyll cells when facing rapid changes in atmospheric moisture (Brodribb et al., 2007; de Boer et al., 2016a; Scoffoni et al., 2017), resulting in a larger change in turgor pressure of guard cells. This might accelerate the transmission of hormonal signal for ABA biosynthesis inside leaves for faster stomatal closure to reduce water loss (Tardieu, 2016; McAdam and Brodribb, 2016; Buckley, 2019) and thus faster stomatal VPD response in these mangrove species. Moreover, epidermal cells of mangroves are smaller than other angiosperms and also smaller than their own stomata (Jiang et al., 2023), meaning that stomata of mangroves have a higher density of peripheral epidermal cells. This design feature might contribute to the stomatal movement as suggested by Gérardin et al. (2018), and thus faster stomatal closure for mangroves. Furthermore, mangroves for the adaptation to super-saline intertidal habitat have evolved a series of water-protection properties, such as highly embolism-resistant xylem (Jiang et al., 2017, 2021, 2022), high hydraulic-capacitance in leaf and root tissues (Aritsara et al., 2022), and strong osmotic regulation (Reef and Lovelock, 2015). They therefore may have enhanced stomatal regulation with a highly sensitive stomatal response to VPD suited to this adaptation to water-deficit prone habitats.

We also found an indirect effect of leaf water status on stomatal dynamics that was mediated mainly by leaf hydraulic traits in our path model. Leaf water status is related to the water absorbed by roots from the soil and water evaporated from stomata into the atmosphere (Cowan, 1965; Buckley, 2019). The water potential in leaf mesophyll and epidermis firstly were reduced after a step increase in VPD, which increased resistance in the leaf water transport (Buckley et al., 2017; Buckley, 2019). As the above results shown in this study that species with more negative leaf predawn water potential (Ψ_{pd}) had more negative P_{12} and P_{50}, and thus regulating stomatal dynamics. For mangroves, the water potential and salinity of the soil and tide determine the water status of leaves in the present study. Thus, although the water potential and salinity of the sites alone cannot explain the mechanism of stomatal VPD response, the continuous pattern of soil-plant hydraulics is often important for understanding how stomatal dynamics are regulated by leaf hydraulic traits (Rodriguez-Dominguez and Brodribb, 2020; Cai et al., 2023).

Our results also showed that the leaves of mangroves had a high bulk modulus of elasticity (ε). This means that cell walls are rigid, and could provide mechanical strength and maintain cellular hydration during dehydration. Our results also showed a negative relationship between C_{leaf} and ε across the mangrove species. This finding was consistent with recent framework on water movements and storage dynamics (Xiong and Nadal, 2020), suggesting that a tight coordination between capacitance and resistance to deformation and shrinkage under tension. Our results also showed that high operating initial steady-state g_s ($g_{s\text{-initial}}$) was closely linked to high leaf hydraulic conductance owing to high vein density in mangroves. This finding is consistent with previous suggestion that a high operating steady-state g_s, resulting from a large aera of leaf-scale stomatal pore, in angiosperms inevitably accelerates transpiratory water loss (Brodribb et al., 2007), which must be supported by water supply of a high vein density (Sack and Frole, 2006; Brodribb et al., 2007). As the path analysis results of the present study found that leaf morphology had an important direct effect on stomatal anatomy, and then had an indirect effect on stomatal dynamics. This is thought to signify the balance between water demand and supply within leaves for mangroves.

5. Conclusions

We provide evidence that stomatal response to a temporal rise in VPD is related directly to stomatal anatomy and hydraulic traits in nine true mangrove species. We also found that the stomata of mangroves have strong sensitivity in response to a step rise in VPD. Faster stomatal closure would be a strategy for conservation water during atmospheric drought, although with higher capacitance and greater embolism resistance of mangrove leaves than those of glycophytic plants. This regulation behavior is suitable for adaptation to water-deficit prone habitats and may improve the advantage of survival in rising global VPD in the future for mangroves. Besides passive stomatal control through hydraulic feedback, the active regulation appears to play a key role in stomatal closure under water deficit in mangroves. A quantitative analysis of both passive and active stomatal regulation behavior is urgently needed for plants living in stressful habitats and confronting with the changing environment.

CRediT authorship contribution statement

Ya-Dong Qie: Writing – review & editing, Writing – original draft, Software, Resources, Project administration, Methodology, Investigation, Formal analysis, Data curation, Conceptualization. **Qi-Wei Zhang:** Writing – review & editing, Visualization, Software, Methodology, Investigation, Formal analysis, Conceptualization. **Scott A.M. McAdam:** Writing – review & editing, Visualization, Validation, Methodology, Formal analysis, Conceptualization. **Kun-Fang Cao:** Writing – review & editing, Visualization, Validation, Supervision, Resources, Project administration, Funding acquisition, Data curation, Conceptualization.

Declaration of competing interest

The authors declare no conflict of interest.

Acknowledgements

We acknowledge the collaboration of the Dongzhaigang National Nature Reserve and Qinglan Harbor Provincial Mangrove Nature Reserve, and the Forestry Department of the Hainan Province for permission to conduct the field experiment in the mangrove reserves. The authors thank Prof. Jun-Jie Zhu for the experimental design, Yang Wei for field assistance, Jin-Yan Lei and Pei-Xin Cui for their help in leaf anatomy. This study was financially supported by a grant of the National Natural Science Foundation of China (31670406) and the Bagui Fellow scholarship (C33600992001) of Guangxi Zhuang Autonomous Region to KFC.

Appendix A. Supplementary data

Supplementary data to this article can be found online at https://doi.org/10.1016/j.pld.2024.02.003.

References

Agduma, A.R., Jiang, X., Liang, D.M., et al., 2022. Stem hydraulic traits are decoupled from leaf ecophysiological traits in mangroves in Southern Philippines. J. Plant Biol. 65, 389–401.
Aritsara, A.N.A., Wang, S., Li, B.N., et al., 2022. Divergent leaf and fine root "pressure–volume relationships" across habitats with varying water availability. Plant Physiol. 190, 2246–2259.
Bao, S.D., 2000. Soil and Agricultural Chemistry Analysis. China Agriculture Press, Beijing.
Beaulieu, J.M., Leitch, I.J., Patel, S., et al., 2008. Genome size is a strong predictor of cell size and stomatal density in angiosperms. New Phytol. 179, 975–986.
Beckett, H.A., Bryant, C., Neeman, T., et al., 2024. Plasticity in branch water relations and stem hydraulic vulnerability enhances hydraulic safety in mangroves

growing along a salinity gradient. Plant Cell Environ. 47, 854–870. https://doi.org/10.1111/pce.14764.
Brodribb, T.J., Field, T.S., Jordan, G.J., 2007. Leaf maximum photosynthetic rate and venation are linked by hydraulics. Plant Physiol. 144, 1890–1898.
Brodribb, T.J., Holbrook, N.M., 2003. Stomatal closure during leaf dehydration, correlation with other leaf physiological traits. Plant Physiol. 132, 2166–2173.
Brodribb, T.J., McAdam, S.A., Jordan, G.J., et al., 2014. Conifer species adapt to low-rainfall climates by following one of two divergent pathways. Proc. Natl. Acad. Sci. U.S.A. 111, 14489–14493.
Brodribb, T.J., McAdam, S.A., 2011. Passive origins of stomatal control in vascular plants. Science 331, 1197985.
Buckley, T.N., John, G.P., Scoffoni, C., et al., 2017. The sites of evaporation within leaves. Plant Physiol. 173, 1763–1782.
Buckley, T.N., Mott, K.A., 2002. Stomatal water relations and the control of hydraulic supply and demand. Prog. Bot. 63, 309–325.
Buckley, T.N., 2019. How do stomata respond to water status? New Phytol. 224, 21–36.
Buckley, T.N., 2016. Stomatal responses to humidity: has the 'black box' finally been opened? Plant Cell Environ. 39, 482–484.
Buckley, T.N., 2005. The control of stomata by water balance. New Phytol. 168, 275–292.
Cai, G.C., Carminati, A., Gleason, S.M., et al., 2023. Soil-plant hydraulics explain stomatal efficiency-safety tradeoff. Plant Cell Environ. 46, 3120–3127.
Chen, X.Y., 2020. Relationship between Leaf Anatomical Structure and Photosynthetic Capacity of Mangrove Plants in Hainan. Guangxi University, Nanning, China.
Choat, B., Brodribb, T.J., Brodersen, C.R., et al., 2018. Triggers of tree mortality under drought. Nature 28, 531–539.
Cowan, I.R., 1965. Transport of water in the soil-plant-atmosphere continuum. J. Appl. Ecol. 2, 221–239.
Cowan, I.R., 1977. Stomatal behaviour and environment. Adv. Bot. Res. 4, 117–228.
Darwin, F., 1898. Observations on stomata. Philos. Trans. R. Soc. Lond. B-Biol. Sci. 190, 531–621.
de Boer, H.J., Drake, P.L., Wendt, E., et al., 2016a. Apparent overinvestment in leaf venation relaxes leaf morphological constraints on photosynthesis in arid habitats. Plant Physiol. 172, 2286–2299.
de Boer, H.J., Price, C.A., Wagner-Cremer, F., et al., 2016b. Optimal allocation of leaf epidermal area for gas exchange. New Phytol. 210, 1219–1228.
Drake, P.L., Froend, R.H., Franks, P.J., 2013. Smaller, faster stomata: scaling of stomatal size, rate of response, and stomatal conductance. J. Exp. Bot. 64, 495–505.
Duke, N.C., Ball, M.C., Ellison, J.C., 1998. Factors influencing biodiversity and distributional gradients in mangroves. Global Ecol. Biogeogr. Lett. 7, 27–47.
Durand, M., Brendel, O., Buré, C., et al., 2019. Altered stomatal dynamics induced by changes in irradiance and vapour-pressure deficit under drought: impacts on the whole-plant transpiration efficiency of poplar genotypes. New Phytol. 222, 1789–1802.
Elliott-Kingston, C., Haworth, M., Yearsley, J.M., et al., 2016. Does size matter? Atmospheric CO_2 may be a stronger driver of stomatal closing rate than stomatal size in taxa that diversified under low CO_2. Front. Plant Sci. 7, e1253.
Fu, X.L., Meinzer, F.C., Woodruff, D.R., et al., 2019. Coordination and trade-offs between leaf and stem hydraulic traits and stomatal regulation along a spectrum of isohydry to anisohydry. Plant Cell Environ. 42, 2245–2258.
Gauthey, A., Backes, D., Balland, J., et al., 2022. The role of hydraulic failure in a massive mangrove die-off event. Front. Plant Sci. 13, 822136.
Gérardin, T., Douthe, C., Flexas, J., et al., 2018. Shade and drought growth conditions strongly impact dynamic responses of stomata to variations in irradiance in *Nicotiana tabacum*. Environ. Exp. Bot. 153, 188–197.
Han, S.M., 2011. Study on Landscape Pattern Dynamics and Driving Forces in Mangroves Wetlands of Dongzhaigang Harbour, Hainan Province. Ph.D. thesis, Beijing Forest University, Beijing, China.
He, Z.W., Feng, X., Chen, Q.P., et al., 2022. Evolution of coastal forests based on a full set of mangrove genomes. Nat. Ecol. Evol. 6, 738–1749.
Henry, C., John, G.P., Pan, R.H., et al., 2019. A stomatal safety-efficiency trade-off constrains responses to leaf dehydration. Nat. Commun. 10, 3398.
Hu, M.J., Sun, W.H., Tsai, W.C., et al., 2020. Chromosome-scale assembly of the *Kandelia obovata* genome. Hortic. Res. 7, 75.
Jalakas, P., Takahashi, Y., Waadt, R., et al., 2021. Molecular mechanisms of stomatal closure in response to rising vapour pressure deficit. New Phytol. 232, 468–475.
Jiang, G.F., Goodale, U.M., Liu, Y.Y., et al., 2017. Salt management strategy defines the stem and leaf hydraulic characteristics of six mangrove tree species. Tree Physiol. 37, 389–401.
Jiang, G.F., Li, S.Y., Li, Y.C., et al., 2022. Coordination of hydraulic thresholds across roots, stems, and leaves of two co-occurring mangrove species. Plant Physiol. 189, 2159–2174.
Jiang, G.F., Li, S.Y., Dinnage, R., et al., 2023. Diverse mangroves deviate from other angiosperms in their genome size, leaf cell size and cell packing density relationships. Ann. Bot. 131, 347–360.
Jiang, X., 2021. Xylem Hydraulic Structure and Function in Mangroves. Ph.D. thesis, Guangxi University, Nanning, China.
Jiang, X., Choat, B., Zhang, Y.J., et al., 2021. Variation in xylem hydraulic structure and function of two mangrove species across a latitudinal gradient in Eastern Australia. Water 13, 850.
Lawson, T., Vialet-Chabrand, S., 2019. Speedy stomata, photosynthesis and plant water use efficiency. New Phytol. 221, 93–98.
Leng, B., 2020. Transpriational Water Consumption and its Influencing Factors in Mangroves of Intertidal Zone. Ph.D. thesis, Guangxi University, Nanning, China.
Martins, S.C.V., McAdam, S.A.M., Deans, R.M., et al., 2016. Stomatal dynamics are limited by leaf hydraulics in ferns and conifers: results from simultaneous measurements of liquid and vapour fluxes in leaves. Plant Cell Environ. 39, 694–705.
Martin-StPaul, N., Delzon, S., Cochard, H., 2017. Plant resistance to drought depends on timely stomatal closure. Ecol. Lett. 20, 1437–1447.
McAdam, S.A.M., Brodribb, T.J., 2015. The evolution of mechanisms driving the stomatal response to vapor pressure deficit. Plant Physiol. 167, 833–843.
McAdam, S.A.M., Brodribb, T.J., 2016. Linking turgor with ABA biosynthesis: implications for stomatal responses to vapor pressure deficit across land plants. Plant Physiol. 171, 2008–2016.
McAusland, L., Vialet-Chabrand, S., Davey, P., et al., 2016. Effects of kinetics of light-induced stomatal responses on photosynthesis and water-use efficiency. New Phytol. 211, 1209–1220.
Meinzer, F.C., 1993. Stomata1 control of transpiration. Tree 8, 289–294.
Meinzer, F.C., Smith, D.D., Woodruff, D.R., et al., 2017. Stomatal kinetics and photosynthetic gas exchange along a continuum of isohydric to anisohydric regulation of plant water status. Plant Cell Environ. 40, 1618–1628.
Peak, D., Mott, K.A., 2011. A new, vapour-phase mechanism for stomatal responses to humidity and temperature. Plant Cell Environ. 34, 162–178.
Raven, J.A., 2014. Speedy small stomata? J. Exp. Bot. 65, 1415–1424.
Reef, R., Lovelock, C.E., 2015. Regulation of water balance in mangroves. Ann. Bot. 115, 385–395.
Rockwell, F.E., Holbrook, N.M., Stroock, A.D., 2014. The competition between liquid and vapor transport in transpiring leaves. Plant Physiol. 164, 1741–1758.
Rodriguez-Dominguez, C.M., Brodribb, T.J., 2020. Declining root water transport drives stomatal closure in olive under moderate water stress. New Phytol. 225, 126–134.
Sack, L., Frole, K., 2006. Leaf structural diversity is related to hydraulic capacity in tropical rainforest trees. Ecology 87, 483–491.
Sack, L., Holbrook, N.M., 2006. Leaf hydraulics. Annu. Rev. Plant Biol. 57, 361–381.
Sack, L., Pasquet-Kok, J., Bartlett, M., 2011. Leaf pressure-volume curve parameters. PrometheusWiki. Available at: https://prometheusprotocols.net/function/water-relations/pressure-volume-curves/leaf-pressure-volume-curve-parameters.
Scoffoni, C., Albuquerque, C., Brodersen, C.R., et al., 2017. Outside-xylem vulnerability, not xylem embolism, controls leaf hydraulic decline during dehydration. Plant Physiol. 173, 1197–1210.
Scoffoni, C., McKown, A.D., Rawls, M., et al., 2012. Dynamics of leaf hydraulic conductance with water status: quantification and analysis of species differences under steady state. J. Exp. Bot. 63, 643–658.
Simonin, K.A., Roddy, A.B., 2018. Genome downsizing, physiological novelty, and the global dominance of flowering plants. PLoS Biology 16, e2003706.
Skelton, R.P., Brodribb, T.J., McAdam, S.A., et al., 2017. Gas exchange recovery following natural drought is rapid unless limited by loss of leaf hydraulic conductance: evidence from an evergreen woodland. New Phytol. 215, 1399–1412.
Skelton, R.P., Dawson, T.E., Thompson, S.E., et al., 2018. Low vulnerability to xylem embolism in leaves and stems of North American oaks. Plant Physiol. 177, 1066–1077.
Sperry, J.S., 2000. Hydraulic constraints on plant gas exchange. Agric. For. Meteorol. 104, 13–23.
Tardieu, F., 2016. Too many partners in root–shoot signals. Does hydraulics qualify as the only signal that feeds back over time for reliable stomatal control? New Phytol. 212, 954–963.
Trueba, S., Pan, R.H., Scoffoni, C., et al., 2019. Thresholds for leaf damage due to dehydration: declines of hydraulic function, stomatal conductance and cellular integrity precede those for photochemistry. New Phytol. 223, 134–149.
Tyree, M.T., Hammel, H.T., 1972. The measurement of the turgor pressure and the water relations of plants by the pressure-bomb technique. J. Exp. Bot. 23, 267–282.
Vialet-Chabrand, S., Dreyer, E., Brendel, O., 2013. Performance of a new dynamic model for predicting diurnal time courses of stomatal conductance at the leaf level. Plant Cell Environ. 36, 1529–1546.
Xiong, D.L., Nadal, M., 2020. Linking water relations and hydraulics with photosynthesis. Plant J. 101, 800–815.